ACS APPLIED MATERIALS & INTERFACES

Research Article

www.acsami.org

"Signal-On" Photoelectrochemical Sensing Strategy Based on Target-Dependent Aptamer Conformational Conversion for Selective Detection of Lead(II) Ion

Yang Zang, Jianping Lei,* Qing Hao, and Huangxian Ju

State Key Laboratory of Analytical Chemistry for Life Science, School of Chemistry and Chemical Engineering, Nanjing University, Nanjing 210093, People's Republic of China

ABSTRACT: A "signal-on" photoelectrochemical sensing strategy for selective determination of Pb^{2+} is designed on the basis of the combination of Pb^{2+}-induced conformational conversion, the amplified effect of reduced graphene oxide (RGO) and resonance energy transfer between CdS quantum dots (QDs) and gold nanoparticles (AuNPs). The RGO/CdS/aptamer platform is constructed via a stepwise modification method, and characterized by electrochemical impedance spectroscopy. In the absence of Pb^{2+}, the AuNP-labeled DNA, as a signal quenching element, can be introduced by hybridization with aptamer on the surface of sensing platform, which quenches the photocurrent of QDs via an energy transfer process. Upon addition of Pb^{2+}, the aptamer is induced into a G-quadruplex structure, which can greatly hinder the hybridization between aptamer and AuNP-labeled DNA due to the competitive occupation of binding sites and steric effect, leading to the recovery of photocurrent. Under optimized conditions, this "signal-on" photoelectrochemical biosensor shows a linear relationship between photocurrent variation and the logarithm of Pb^{2+} concentration in the range of 0.1−50 nM with a detection limit of 0.05 nM. Meanwhile, it also exhibits good selectivity for Pb^{2+} over other interfering ions, and is successfully applied to the detection of Pb^{2+} in environmental water samples. By substituting the aptamers with other sequences, this proposed strategy could be conveniently extended to detect different targets as versatile photoelectrochemical devices.

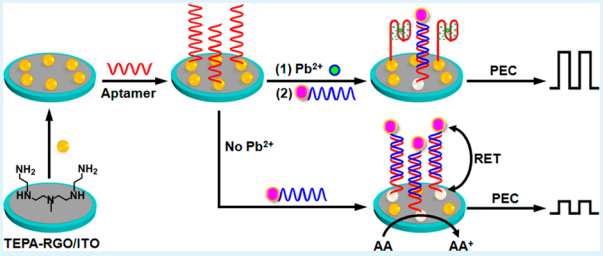

KEYWORDS: *photoelectrochemistry, biosensors, quantum dots, aptamer, resonance energy transfer, detection*

INTRODUCTION

Lead ions (Pb^{2+}) are a major and persistent environmental pollutant that could cause severe health risks.[1,2] Exposure of Pb^{2+} to humans can present serious hazards to the brain, kidneys, and nervous system.[3,4] The conventional analytical techniques including atomic absorption spectrometry, mass spectrometry and atomic emission spectrometry, suffer from the sophisticated instruments and complicated operation in the detection of Pb^{2+}. To solve these problems, several promising measurements have been applied to monitor the levels of Pb^{2+} such as fluorescence,[5−7] electrochemistry,[8,9] electrochemiluminescence,[10,11] colorimetry,[12,13] and surface plasmon resonance.[14] These techniques show good performance in the detection of Pb^{2+}; however, the applications of these techniques are limited due to low selectivity and high cost of measurements. Therefore, designing a novel determination method for sensitive Pb^{2+} is still a challenge.

Photoelectrochemistry (PEC), in which the light is used as the excitation source and a photocurrent is used as the detection signal, has received substantial attention owing to its low background signal and desirable sensitivity.[15−17] In particular, quantum dots (QDs)-based photoelectrochemistry has been extensively applied to bioanalysis due to the resistance to photobleaching[18] and high efficiency of charge separation.[19] The conventional methods of photoelectrochemistry often rely on steric hindrance during biorecognition reactions,[20] generation/consumption of coreactant[21−23] and resonance energy transfer (RET).[24] Among them, RET is a powerful strategy for sensitive detection of DNA binding events via energy transfer between energy donors and acceptors at certain distance. For example, a photoelectrochemical detection system based on energy transfer between CdS QDs and gold nanoparticles (AuNPs) was used for the sensitive biosensing of DNA with a detection limit of 2.0 fM.[25] Therefore, coupling with the energy transfer between AuNPs and QDs, a sensitive photoelectrochemical strategy can be designed for Pb^{2+} assay.

The G-quadruplex aptamer, generally stabilized by metal cations (such as K^+ and Pb^{2+}), has emerged as a specific identification element to build elegant and versatile devices.[26−28] In contrast to K^+, Pb^{2+} has a higher G-quadruplex-stabilizing efficiency resulted from the formation of a more compact structure. Li and co-workers have reported a Pb^{2+}-driven DNA molecular device by means of duplex−quadruplex exchange, which reveals that the stability of the duplex is lower than that of the Pb^{2+}-induced G-quadruplex structure and higher than that of K^+-driven G-quadruplex DNA under certain

Received: June 15, 2014
Accepted: August 29, 2014
Published: August 29, 2014

conditions.[29,30] A sensitive photoelectrochemical sensing was achieved for the detection of Pb^{2+} by using the K^+-stabilized G-quadruplex structure and biocatalytic precipitation.[31] To further improve the sensitivity, it is desirable to employ reduced graphene oxide (RGO) as supporter for the development of the competitive photoelectrochemical sensing platform based on the conformational conversion of duplex−quadruplex.

Reduced graphene oxide has often been used in electrochemical and photoelectrochemical sensors owing to excellent conductivity and large surface area.[32−35] In particular, tetraethylene pentamine (TEPA)-functionalized RGO introduces a large number of amino groups, which are beneficial to the electrostatic modification of thioglycolic acid-stabilized CdS QDs and the enhancement of photocurrent response.[36] In this work, by integrating the competitive interaction of aptamer with Pb^{2+}, signal amplification of RGO, and RET between CdS QDs and AuNPs, a novel photoelectrochemical sensing scaffold was developed for selective detection of Pb^{2+} (Scheme 1). The

Scheme 1. Schematic Diagram for Stepwise Modification of ITO/RGO/CdS/Aptamer Sensing Platform and "Signal-On" Photoelectrochemical Detection Strategy of Pb^{2+} on the basis of Duplex−Quadruplex Conversion and RET Process between CdS QDs and AuNPs

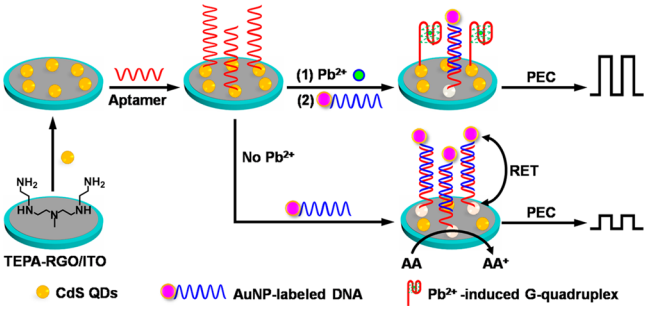

photoelectrochemical sensor was efficiently constructed by stepwise assembly of TEPA-functionalized RGO and thioglycolic acid-stabilized CdS QDs via electrostatic interaction, followed by the covalent interaction of aptamer via amide reaction. Under irradiation, QDs can generate electron−hole pairs while ascorbic acid (AA), as a sacrificial electron donor, is easily oxidized by photogenerated holes, and results in a stable anodic photocurrent. In the absence of Pb^{2+}, the AuNP-labeled DNA, as a signal quenching element, can be introduced onto the surface of sensing platform by hybridization with aptamer, leading to the quenched photocurrent of QDs via energy transfer process. Upon addition of Pb^{2+}, the photocurrent was recovered because Pb^{2+} induced the aptamer into the G-quadruplex structure, which can block the hybridization between aptamer and AuNP-labeled DNA, and thus enhance the photocurrent. By integrating Pb^{2+}-induced G-quadruplex structure and energy transfer between CdS QDs and AuNPs, a "signal-on" photoelectrochemical aptasensor is achieved with good performance, and shows a promising application in clinical and environmental analyses.

EXPERIMENTAL SECTION

Materials and Reagents. An Indium tin oxide (ITO) electrode was purchased from Zhuhai Kaivo Electronic Components Co. Ltd. (China). Thioglycolic acid (TGA), monoethanolamine (MEA), 1-ethyl-3-(3-(dimethylamino)propyl) carbodiimide (EDC), *n*-hydroxysuccinimide (NHS) and tris(2-carboxyethyl)-phosphine hydrochloride (TCEP) were purchased from Sigma-Aldrich. Cadmium chloride ($CdCl_2·2.5H_2O$) was purchased from Alfa Aesar China Ltd. $Na_2S·9H_2O$ was obtained from Shanghai Lingfeng Chemical Reagent Co. Ltd. Chloroauric acid ($HAuCl_4·4H_2O$) was purchased from Nanjing Chemical Reagent Co. Ltd. Sodium borohydride was purchased from Tianjin Chemagent Research Co. Ltd. TEPA-RGO was purchased from XFNANO Materials Tech Co. Ltd. (Nanjing, China). All other chemicals were of analytical grade without further purification. The washing buffer was 10 mM phosphate buffered saline (PBS) of pH 7.4 containing 0.1 M NaCl. All aqueous solutions were prepared using ultrapure water obtained from a Millipore water purification system (≥18 MΩ, Milli-Q, Millipore). All oligonucleotides used in this work were synthesized and purified by Sangon Biological Engineering Technology & Co. Ltd. (Shanghai, China) and the corresponding sequences are summarized below:

Pb^{2+}aptamer: 5′-NH_2-$(CH_2)_6$-TTG GGT GGG TGG GTG GGT-3′

HS-modified DNA: 5′-SH-$(CH_2)_6$-TTT TTT ACC CAC CCA CCC-3′

Apparatus. Transmission electron microscopy (TEM) was conducted using a JEM-2100 microscope (JEOL, Japan). Photoluminescence (PL) was measured using an RF-5301PC fluorescence spectrometer (Shimadzu Co., Japan) equipped with a xenon lamp. UV−vis absorption spectra were obtained using a UV-3600 UV−vis−near-infrared spectrophotometer (Shimadzu, Japan). Dynamic light scattering (DLS) measurements were performed by BI-200 SM light scattering apparatus (Brookhaven Instruments Co., USA) equipped with a digital correlator at 640 nm. The photoelectrochemical measurements were performed on a Zahner PEC workstation (Zahner, German) with a LW405 light as the accessory light source. All experiments were carried out at room temperature using a conventional three-electrode system with a modified ITO electrode (4 mm in diameter) as the working electrode, a platinum wire as the auxiliary electrode, and a saturated calomel as the reference electrode. Electrochemical impedance spectroscopy (EIS) was conducted using an Autolab potentiostat/galvanostat (PGSTAT 30, Eco Chemie B.V., Utrecht, The Netherlands) in 0.1 M Na_2SO_4 solution containing 5 mM $K_4[Fe(CN)_6]/K_3[Fe(CN)_6]$ (1:1) mixture as the redox probe from 0.1 Hz to 100 kHz with a signal amplitude of 5 mV and the applied potential of 0.18 V.

Synthesis of TGA-Capped CdS QDs. CdS QDs were synthesized according to the previous report.[37] Typically, 250 μL of thioglycolic acid was injected into 50 mL of 0.01 M $CdCl_2$(aq), and highly pure N_2 was bubbled for 30 min. After being adjusted to pH 11 with 1.0 M NaOH, 5.0 mL of 0.1 M Na_2S(aq) was injected. The resulting mixture solution was subsequently heated to 110 °C and refluxed for 4 h to obtain TGA-capped water-soluble CdS QDs. Finally, the as-prepared QDs solution was diluted with the same volume of water and kept in a refrigerator at 4 °C. Before usage, this QDs solution was sedimentated with isopropyl alcohol and collected by centrifugation. The colloidal precipitate was then dissolved with an equivalent amount of deionized water for subsequent experiments.

Preparation of AuNP-Labeled DNA. First, AuNPs with average diameter 5 ± 1 nm were prepared according to the procedure of literature.[25] Briefly, 30 μL of 50 μM HS-modified DNA and 15 μL of 10 mM TCEP were mixed and incubated for 30 min at room temperature in order to reduce disulfide bonds. Then, the required amount of AuNPs was added into the above solution to achieve a final DNA concentration of 1 μM and incubated for 16 h at room temperature under gentle shaking and a dark environment. The resultant solution was centrifuged for 30 min at 15000 rpm. After removal of the supernatant, the precipitate was resuspended in 10 mM PBS of pH 7.4 containing 0.1 M NaCl.

Fabrication and Detection Process of Photoelectrochemical Biosensor. The ITO electrode was sequentially cleaned with 1.0 M NaOH and H_2O_2 (10%), washed with acetone and twice-ultrapure water, then dried under N_2 atmosphere. The RGO/CdS modified electrode was prepared through electrostatic interaction. Briefly, 10 μL of 0.5 mg·mL^{-1} RGO stock solution was coated on an ITO electrode surface and dried at room temperature. Then, 10 μL of CdS QDs was

applied to the electrode before being allowed to dry at room temperature. After the electrode was rinsed with PBS and dried under N_2 atmosphere, the RGO/CdS modified ITO electrode was obtained.

Pb^{2+} aptamer was immobilized onto the RGO/CdS modified ITO electrode by amide reaction. First, TGA-capped CdS QDs were activated in 20 μL of 0.01 M PBS buffer (pH 5.3) containing 10 mM EDC and 20 mM NHS for 1 h at room temperature. Then, this activated electrode was rinsed with PBS. Subsequently, 20 μL of 0.2 μM aptamer was applied to the electrode surface and incubated at 4 °C overnight. After incubation, the electrode was washed three times to remove the nonconjugated DNA. Finally, the modified electrode was blocked with 1 mM MEA for 2 h at 4 °C and washed with PBS thoroughly.

To evaluate the detection performance of as-prepared sensor, 20 μL of Pb^{2+} solution of different concentrations was added onto the RGO/CdS/aptamer modified ITO electrode and incubated at room temperature for 0.5 h. Next, 20 μL of AuNP-labeled DNA was applied to the electrode surface and incubated at 37.1 °C for 1.5 h. The modified electrode was washed with PBS and dried under N_2 atmosphere after each modification step. Finally, the electrode was immersed in the electrolyte for photoelectrochemical detection. All photoelectrochemical experiments were measured at a constant potential of −0.15 V in 0.1 M air-saturation PBS of pH 7.4 containing 0.1 M ascorbic acid as a sacrificial electron donor.[38]

RESULTS AND DISCUSSION

Characterization of AuNPs, CdS QDs, RGO, and RGO/CdS Nanocomposites. To acquire the sizes of AuNPs and CdS QDs, TEM was performed and the micrographs are displayed in Figure 1. As shown in Figure 1A, spherical AuNPs

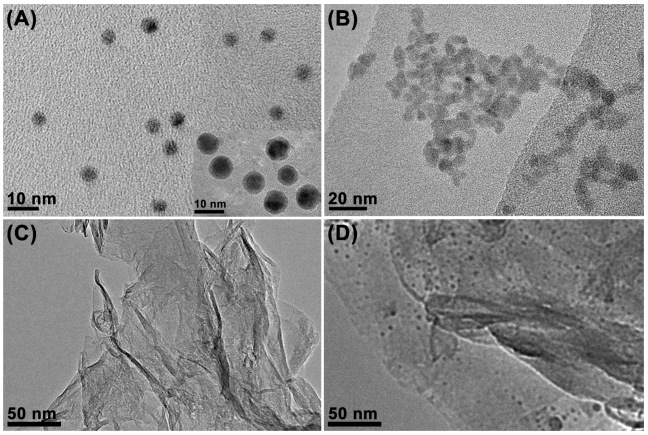

Figure 1. TEM images of (A) AuNPs, (B) CdS QDs, (C) RGO, and (D) RGO/CdS nanocomposites. Inset of panel A is TEM image of DNA/AuNPs.

were homogeneously dispersed with an average size of 5 nm. After the capture DNA was added and assembled , the diameter of capture DNA/AuNPs obviously increased without aggregation (Figure 1A, inset). Figure 1B shows that the CdS QDs were quasi-spherical nanoparticles with the diameters of 5 ± 1 nm. The morphology of RGO and RGO/CdS nanocomposites was also characterized by TEM. RGO sheets had mono- to few-layered structures (Figure 1C), which could provide three-dimensional matrixes to facilitate electron conduction between photoexcited CdS QDs and RGO through wrinkle-induced tunnels. Besides, Figure 1D shows CdS QDs were homogeneously decorated on the surface of RGO sheets. The three-dimensional dispersion of RGO/CdS nanocomposites was beneficial to covalent assembly of Pb^{2+} aptamer and the charge separation of QDs.[33,39,40]

Figure 2A displays the UV−vis absorption spectrum of AuNPs and the PL spectrum of CdS QDs. The maximum

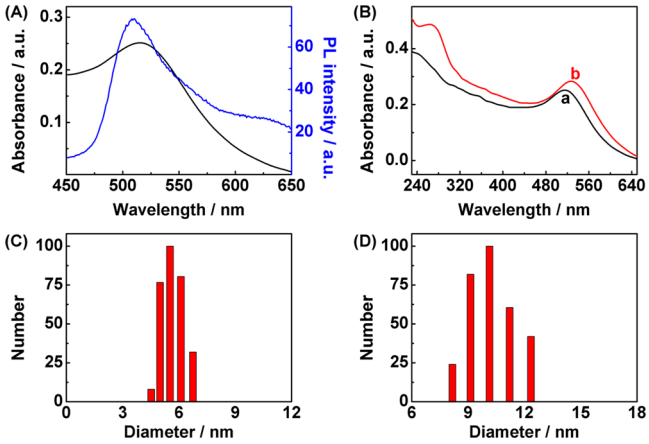

Figure 2. (A) UV−vis absorption spectrum of AuNPs and PL spectrum of CdS QDs (excitation wavelength: 405 nm). (B) UV−vis spectra of AuNPs (a) and AuNP-labeled DNA (b). Particle size distributions of (C) AuNPs and (D) AuNP-labeled DNA suspended in aqueous solution measured by DLS.

plasmon absorption peak of AuNPs was located at ca. 519 nm, whereas the typical PL emission peak of CdS QDs was centered at ca. 510 nm. Obviously, the broad surface plasmon resonance of AuNPs and the PL emission of CdS QDs were overlapped in a wide wavelength range, which provided the possibility for resonance energy transfer.[38]

Meanwhile, to verify the assembly of AuNPs with DNA, the UV−vis spectra of AuNPs and AuNP-labeled DNA were acquired for comparison (Figure 2B). Initially, AuNPs and DNA showed an absorbance peak at 519 and 260 nm originated from conjugated double bond of nucleobases, respectively, as displayed in trace a. After incubating the AuNPs in DNA, the 519 nm absorption peak was observed to have shifted to 527 nm, as shown in trace b, which supports the AuNP−DNA assembly. In addition, the hydrodynamic diameters of AuNPs and AuNP-labeled DNA composites were also measured by DLS. As displayed in Figure 2C, the mean hydrodynamic diameter of AuNPs was 5.8 nm. After decorated with DNA, the resulting hydrodynamic diameter increased to 10.1 nm (Figure 2D), confirming the successful loading of DNA on AuNPs surface.

Feasibility and Stepwise Fabrication of Photoelectrochemical Aptasensor. Figure 3A shows the photocurrent

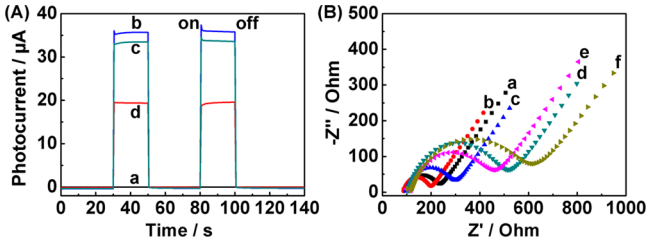

Figure 3. (A) Photocurrent response of the RGO (a), RGO/CdS (b), RGO/CdS/aptamer (c) modified ITO electrodes, and (c) hybridized with AuNP-labeled DNA (d). (B) Impedance spectra of bare ITO (a), RGO (b), RGO/CdS (c), and RGO/CdS/aptamer (d) modified ITO electrodes, (d) blocked by MEA (e), and (e) hybridized with AuNP-labeled DNA (f).

response of different modified electrodes. As displayed in curve a, no photoresponse was observed for RGO modified ITO electrode because RGO could not be excited. With the modification process, the photocurrent increased sharply for RGO/CdS modified ITO electrode (curve b), whereas the photocurrents of the electrodes sequentially modified by Pb^{2+} aptamer and monoethanolamine (curve c), and AuNP-labeled DNA (curve d) were declined due to the steric hindrance of aptamer and inhibition effect of AuNPs, respectively.

The stepwise assembly process of the Pb^{2+} aptasensor was further investigated by electrochemical impedance spectroscopy, which was a powerful tool for describing the interface properties of electrodes. Figure 3B displays the impedance spectra of different modified electrodes related to each construction step of the biosensor. After RGO was coated onto the ITO surface, the impedance spectrum of the RGO modified ITO electrode (curve b) showed a lower charge-transfer resistance (R_{ct}) of 106.9 Ω compared to 133.5 Ω for the ITO electrode (curve a), which was attributed to the excellent electron transfer property of RGO. With the CdS QDs (curve c) and aptamer (curve d) assembled on ITO/RGO electrode, R_{ct} increased significantly to 194.5 and 396.0 Ω, respectively. After blocked by MEA (curve e), the R_{ct} value decreased to 330.9 Ω due to electrostatic interaction between the positively charged MEA and negatively charged redox probe. In contrast, when hybridization of negatively charged AuNP-labeled DNA occurred, R_{ct} value of RGO/CdS/aptamer/AuNP-labeled DNA modified ITO electrode significantly increased to 489.2 Ω (curve f). These results suggested that the photoelectrochemical sensor was constructed as expected, providing a sensitive sensing platform for Pb^{2+} detection.

Optimization of Conditions for Photoelectrochemical Detection. To achieve excellent performance in the photoelectrochemical assay of Pb^{2+}, several experiment parameters such as the amount of RGO for modification, the volume of CdS QDs, the concentration of aptamer and the incubation time of hybridization were optimized in Figure 4. As shown in Figure 4A, the photocurrent intensity increased with the increasing of RGO concentration up to 0.5 mg·mL^{-1} and then slightly decreased as further elevation of the RGO concentration, which was attributed to that the increasing film thickness could block the analyte's diffusion. Thus, 0.5 mg·mL^{-1} of RGO was used for the construction of aptasensor. On the other hand, the dependence of photocurrent intensity on the amount of CdS QDs assembled on ITO electrode was investigated in Figure 4B. When 10 μL of CdS QDs was added, the photocurrent intensity reached the maximum. With further increase of QDs' volume (such as 20 μL), the photocurrent intensity decreased due to the increasing of film thickness that blocked the electron exchange.[21] Therefore, 10 μL was favorable for this system as the optimal volume.

In addition, as a Pb^{2+} recognition probe, the concentration of aptamer dramatically influenced the detection sensitivity of the proposed biosensor. As displayed in Figure 4C, with an increasing concentration of aptamer, the photocurrent intensity gradually declined because it could capture more AuNP-labeled DNA. When aptamer concentration was 0.2 μM, the photocurrent intensity nearly reached a plateau. Thus, 0.2 μM of aptamer was employed for the next experiments. Meanwhile, incubation time between aptamer and AuNP-labeled DNA also affected the performance of this biosensor. As shown in Figure 4D, the desirable photocurrent change was

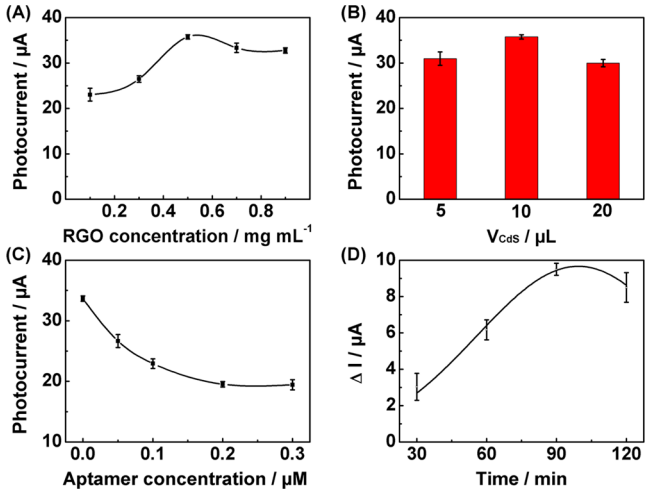

Figure 4. Effects of (A) RGO concentration, and (B) the volume of CdS QDs on photocurrent response at RGO/CdS modified ITO electrode. (C) Plot of photocurrent vs aptamer concentration in the presence of AuNP-labeled DNA at RGO/CdS/aptamer modified ITO electrode. (D) Effect of incubation time between aptamer and AuNP-labeled DNA on photocurrent change of photoelectrochemical aptasensor ($\Delta I = I - I_0$, I and I_0 are the photocurrents of aptasensor with and without 50 nM Pb^{2+}, respectively).

obtained after 1.5 h in the presence of 50 nM Pb^{2+}. To efficiently facilitate photoelectrochemical detection, 1.5 h was selected as the optimal reaction time.

Analytical Performances of Photoelectrochemical Aptasensor. On the basis of the "signal-on" strategy, this as-prepared aptasensor was applied to Pb^{2+} detection as stated above. Figure 5A depicts the photocurrent signals measured at

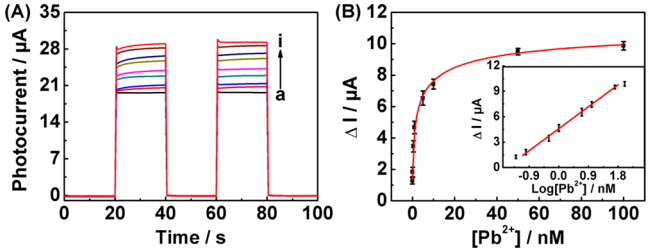

Figure 5. (A) Photocurrent response of the aptasensor at different concentrations of Pb^{2+}: 0 (a), 0.05 (b), 0.1 (c), 0.5 (d), 1.0 (e), 5.0 (f), 10 (g), 50 (h), and 100 nM (i). (B) Plot of photocurrent change vs Pb^{2+} concentration. Inset: calibration curve.

different concentrations of Pb^{2+}. In the absence of Pb^{2+}, a low photocurrent was obtained due to the photoelectrochemical inhibition via energy transfer between QDs and the introduced AuNPs. As the concentration of Pb^{2+} increased, the photocurrent intensity was gradually enhanced. These results showed that the Pb^{2+}-induced G-quadruplex structure was formed and subsequently hindered the hybridization of aptamer with AuNP-labeled DNA.

Figure 5B outlined the relationship between the increment of photocurrent ΔI ($\Delta I = I - I_0$) and logarithm of Pb^{2+} concentration, where I and I_0 were the photocurrent intensities of aptasensor in the presence and absence of Pb^{2+}. A linear range was determined to be 0.1−50 nM. The regression equation was ΔI (μA) = 4.59 + 2.87 log [Pb^{2+}] (nM) with the correlation coefficient of 0.998 (Figure 5B, inset). The limit of

dx.doi.org/10.1021/am503804g | ACS Appl. Mater. Interfaces 2014, 6, 15991−15997

Table 1. Comparison of Various Pb^{2+} Biosensors Based on Pb^{2+}-Dependent DNAzyme

detection method	LOD (nM)	linear range (nM)	ref
photoelectrochemical detection based on energy transfer using RGO/CdS/aptamer and AuNPs	0.05	0.1−50	this work
photoelectrochemical sensor via G-quadruplex DNAzyme-related biocatalytic precipitation	10	50−10000	31
photoelectrochemical sensor based on ZnO nanoflower/Pb^{2+}-dependent DNAzyme	0.1	0.5−20	41
fluorescence detection via the energy transfer from G-quadruplex-labeled CdSe/ZnS to graphene oxide	0.09	0.1−10	42
amplified fluorescence biosensor using graphene and DNAzyme	0.3	1.0−100	43
electrochemical detection by an electrode-bound DNAzyme assembly	300	500−10000	44
electrochemical DNAzyme sensor coupling with an amplification of DNA-Au biobar codes	1.0	5.0−100	45
electrochemiluminescence detection on the basis of Pb^{2+}-dependent DNAzyme	0.011	0.25−1.0	46
DLS detection using Pb^{2+}-dependent DNAzyme and AuNPs probes	0.035	0.1−1.0	47

detection (LOD) of 0.05 nM for Pb^{2+} was achieved at 3σ. For comparison, the analytical characteristics of several Pb^{2+} biosensors based on Pb^{2+}-dependent DNAzyme are presented in Table 1. Apparently, the LOD of our sensing device was lower than most of photoelectrochemical, fluorescent and electrochemical methods that reported previously. Moreover, this proposed sensor had acceptable linear range owing to the efficient charge-separation of RGO/CdS and quenching effect of AuNPs.

To evaluate the selectivity of the designed strategy for Pb^{2+} assay, the photocurrent response of this system was investigated against other common metal ions including Na^+, K^+, Zn^{2+}, Ni^{2+}, Fe^{3+}, Co^{2+}, Al^{3+}, and Mg^{2+} ions. As shown in Figure 6A, no

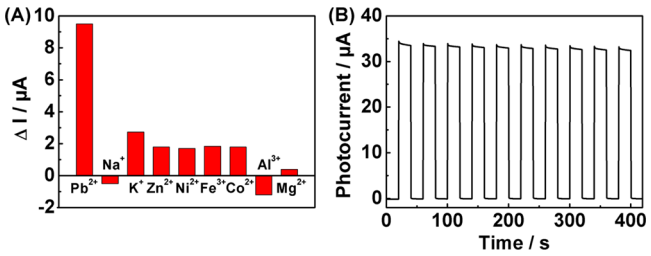

Figure 6. (A) Photocurrent changes of the prepared aptasensor toward 50 nM Pb^{2+} against 500 nM other metal ions. (B) Time-based photocurrent response of RGO/CdS/aptamer modified ITO electrode.

significant photocurrent change was observed upon the addition of 10-fold excess of other interfering ions in comparison with Pb^{2+}. Although K^+ could also induce G-quadruplex conversion, only a minor increase of photocurrent was observed after adding K^+ compared with other interfering ions, which revealed the different structural stability between K^+-induced and Pb^{2+}-induced G-quadruplexes.[48] Thus, the proposed system showed high selectivity against interfering ions for Pb^{2+} detection.

Stability is also an important parameter in evaluating the performance of the aptasensor. Figure 6B displays the time-based photocurrent response of the RGO/CdS/aptamer modified ITO electrode, which was generated periodically as the light switched every 20 s. As the light was turned on, the electrode showed a strong and fairly stable photocurrent response. Moreover, this aptasensor for Pb^{2+} exhibited good fabrication reproducibility with a relative standard deviation of 4.6% for five freshly prepared RGO/CdS/aptamer modified ITO electrodes. When it was not in use, the sensor was stored in dark conditions at 4 °C. The photocurrent response had no obvious change after storage for 10 days, showing good stability and detection reliability.

Detection of Pb^{2+} in Environmental Water Samples. To evaluate the applicability of the present system, the sensor is used for quantifying the Pb^{2+} in tap water and lake water. The lake water was from the Xuanwu Lake Park (Nanjing, Jiangsu province, China) and filtered through 0.22 μm ultrafiltration membrane before detection. As shown in Table 2, the Pb^{2+} concentrations detected by photoelectrochemical method were 0.19 nM and 0.43 nM for tap and lake water, respectively. When spiked with 5, 10, and 20 nM Pb^{2+} standard solutions, the average recoveries for three photoelectrochemical detections ranged from 95.2% to 105.4%, showing good accuracy and acceptable precision.

Table 2. Detection Results and Recoveries of Pb^{2+} in Environmental Water Samples Using the Proposed Photoelectrochemical Sensor

sample	added (nM)	found (nM)[a]	recovery (%)
tap water	0	0.19 ± 0.04	
	5	5.47 ± 0.15	105.4
	10	9.70 ± 0.17	95.2
	20	20.6 ± 0.32	102.0
lake water	0	0.43 ± 0.05	
	5	5.23 ± 0.21	96.3
	10	10.7 ± 0.26	102.6
	20	21.2 ± 0.20	103.8

[a]Mean of three photoelectrochemical measurements ± standard deviation.

CONCLUSION

A "signal-on" photoelectrochemical strategy was successfully designed for Pb^{2+} assay based on target-induced duplex−quadruplex conversion. The photoelectrochemical sensing platform of the RGO/CdS/aptamer modified ITO electrode was conveniently constructed though a stepwise modification method. The introduction of RGO is not only beneficial to the immobilization of QDs via electrostatic interaction but also efficient to capture and transport of photoelectrons, leading to the improvement of photocurrent response. In the absence of Pb^{2+}, the photocurrent of QDs was quenched via resonance energy transfer when the aptamer was hybridized with AuNP-labeled DNA as signal quenching element on the sensing surface. Because the Pb^{2+}-induced G-quadruplex structure has higher stability than that of the duplex, the hybridization of the aptamer with AuNP-labeled DNA could be hindered in the presence of Pb^{2+}, leading to the recovery of the photocurrent. By integrating Pb^{2+}-induced G-quadruplex structure conversion and energy transfer between CdS QDs and AuNPs, this aptasensor exhibited high sensitivity, acceptable linear range,

good selectivity and excellent stability. Furthermore, this method had been applied successfully to detect Pb^{2+} in real samples owing to its resistance to environmental interferes. The DNAzyme-based photoelectrochemical strategy endows the new concept of sensing device, and could expand the application range of photoelectrochemical aptasensor in analytical fields.

AUTHOR INFORMATION

Corresponding Author

*J. Lei. Phone/Fax: +86-25-83593593. E-mail: jpl@nju.edu.cn.

Notes

The authors declare no competing financial interest.

ACKNOWLEDGMENTS

We gratefully acknowledge National Basic Research Program (2010CB732400) and National Natural Science Foundation of China (21375060, 21135002, 21121091).

REFERENCES

(1) Marbella, L.; Serli-Mitasev, B.; Basu, P. Development of a Fluorescent Pb^{2+} Sensor. *Angew. Chem., Int. Ed.* **2009**, *48*, 3996−3998.

(2) Sadrolhosseini, A. R.; Noor, A. S. M.; Bahrami, A.; Lim, H. N.; Talib, Z. A.; Mahdi, M. A. Application of Polypyrrole Multi-Walled Carbon Nanotube Composite Layer for Detection of Mercury, Lead and Iron Ions Using Surface Plasmon Resonance Technique. *PLoS One* **2014**, *9*, e93962.

(3) Goyer, R. A. Lead Toxicity: Current Concerns. *Environ. Health Perspect.* **1993**, *100*, 177−187.

(4) Lin, Z. Z.; Li, X. H.; Kraatz, H. B. Impedimetric Immobilized DNA-based Sensor for Simultaneous Detection of Pb^{2+}, Ag^{+}, and Hg^{2+}. *Anal. Chem.* **2011**, *83*, 6896−6901.

(5) Li, C. L.; Liu, K. T.; Lin, Y. W.; Chang, H. T. Fluorescence Detection of Lead(II) Ions Through Their Induced Catalytic Activity of DNAzymes. *Anal. Chem.* **2011**, *83*, 225−230.

(6) He, H. Z.; Leung, K. H.; Yang, H.; Chan, D. S. H.; Leung, C. H.; Zhou, J.; Bourdoncle, A.; Mergny, J. L.; Ma, D. L. Label-Free Detection of Sub-Nanomolar Lead(II) Ions in Aqueous Solution Using a Metal-based Luminescent Switch-On Probe. *Biosens. Bioelectron.* **2013**, *41*, 871−874.

(7) Wen, Y. Q.; Peng, C.; Li, D.; Zhuo, L.; He, S. J.; Wang, L. H.; Huang, Q.; Xu, Q. H.; Fan, C. H. Metal Ion-Modulated Graphene-DNAzyme Interactions: Design of a Nanoprobe for Fluorescent Detection of Lead(II) Ions with High Sensitivity, Selectivity and Tunable Dynamic Range. *Chem. Commun.* **2011**, *47*, 6278−6280.

(8) Su, W. Q.; Cho, M.; Nam, J. D.; Choe, W. S.; Lee, Y. Highly Sensitive Electrochemical Lead Ion Sensor Harnessing Peptide Probe Molecules on Porous Gold Electrodes. *Biosens. Bioelectron.* **2013**, *48*, 263−269.

(9) Wang, B.; Luo, B.; Liang, M. H.; Wang, A.; Wang, J.; Fang, Y.; Chang, Y. H.; Zhi, L. J. Chemical Amination of Graphene Oxides and Their Extraordinary Properties in the Detection of Lead Ions. *Nanoscale* **2011**, *3*, 5059−5066.

(10) Dong, Y. Q.; Tian, W. R.; Ren, S. Y.; Dai, R. P.; Chi, Y. W.; Chen, G. N. Graphene Quantum Dots/L-Cysteine Coreactant Electrochemiluminescence System and Its Application in Sensing Lead(II) Ions. *ACS Appl. Mater. Interfaces* **2014**, *6*, 1646−1651.

(11) Gao, A.; Tang, C. X.; He, X. W.; Yin, X. B. Electrochemiluminescent Lead Biosensor Based on GR-5 Lead-Dependent DNAzyme for $Ru(phen)_3^{2+}$ Intercalation and Lead Recognition. *Analyst* **2013**, *138*, 263−268.

(12) Ferhan, A. R.; Guo, L. H.; Zhou, X. D.; Chen, P.; Hong, S.; Kim, D. H. Solid-Phase Colorimetric Sensor Based on Gold Nanoparticle-Loaded Polymer Brushes: Lead Detection as a Case Study. *Anal. Chem.* **2013**, *85*, 4094−4099.

(13) Yan, J.; Indra, E. M. Colorimetric Method for Determining Pb^{2+} Ions in Water Enhanced with Non-Precious-Metal Nanoparticles. *Anal. Chem.* **2012**, *84*, 6122−6127.

(14) Pelossof, G.; Tel-Vered, R.; Willner, I. Amplified Surface Plasmon Resonance and Electrochemical Detection of Pb^{2+} Ions Using the Pb^{2+}-Dependent DNAzyme and Hemin/G-Quadruplex as a Label. *Anal. Chem.* **2012**, *84*, 3703−3709.

(15) Long, Y. T.; Kong, C.; Li, D. W.; Li, Y.; Chowdhury, S.; Tian, H. Ultrasensitive Determination of Cysteine Based on the Photocurrent of Nafion-Functionalized CdS−MV Quantum Dots on an ITO Electrode. *Small* **2011**, *7*, 1624−1628.

(16) Lu, W.; Jin, Y.; Wang, G.; Chen, D.; Li, J. H. Enhanced Photoelectrochemical Method for Linear DNA Hybridization Detection Using Au-Nanopaticle Labeled DNA as Probe onto Titanium Dioxide Electrode. *Biosens. Bioelectron.* **2008**, *23*, 1534−1539.

(17) Chen, D.; Zhang, H.; Li, X.; Li, J. H. Biofunctional Titania Nanotubes for Visible-Light-Activated Photoelectrochemical Biosensing. *Anal. Chem.* **2010**, *82*, 2253−2261.

(18) Gill, R.; Zayats, M.; Willner, I. Semiconductor Quantum Dots for Bioanalysis. *Angew. Chem., Int. Ed.* **2008**, *47*, 7602−7625.

(19) Zhang, X. R.; Li, S. G.; Jin, X.; Zhang, S. S. A New Photoelectrochemical Aptasensor for the Detection of Thrombin Based on Functionalized Graphene and CdSe Nanoparticles Multilayers. *Chem. Commun.* **2011**, *47*, 4929−4931.

(20) Haddour, N.; Chauvin, J.; Gondran, C.; Cosnier, S. Photoelectrochemical Immunosensor for Label-Free Detection and Quantification of Anti-Cholera Toxin Antibody. *J. Am. Chem. Soc.* **2006**, *128*, 9693−9698.

(21) Wang, W. J.; Hao, Q.; Wang, W.; Bao, L.; Lei, J. P.; Wang, Q. B.; Ju, H. X. Quantum Dot-Functionalized Porous ZnO Nanosheets as a Visible Light Induced Photoelectrochemical Platform for DNA Detection. *Nanoscale* **2014**, *6*, 2710−2717.

(22) Wang, M.; Yin, H. S.; Shen, N. N.; Xu, Z. N.; Sun, B.; Ai, S. Y. Signal-On Photoelectrochemical Biosensor for MicroRNA Detection Based on Bi_2S_3 Nanorods and Enzymatic Amplification. *Biosens. Bioelectron.* **2014**, *53*, 232−237.

(23) Tanne, J.; Schäfer, D.; Khalid, W.; Parak, W. J.; Lisdat, F. Light-Controlled Bioelectrochemical Sensor Based on CdSe/ZnS Quantum Dots. *Anal. Chem.* **2011**, *83*, 7778−7785.

(24) Zhang, X. R.; Xu, Y. P.; Yang, Y. Q.; Jin, X.; Ye, S. J.; Zhang, S. S.; Jiang, L. L. A New Signal-On Photoelectrochemical Biosensor Based on a Graphene/Quantum-Dot Nanocomposite Amplified by the Dual-Quenched Effect of Bipyridinium Relay and AuNPs. *Chem.—Eur. J.* **2012**, *18*, 16411−16418.

(25) Zhao, W. W.; Wang, J.; Xu, J. J.; Chen, H. Y. Energy Transfer Between CdS Quantum Dots and Au Nanoparticles in Photoelectrochemical Detection. *Chem. Commun.* **2011**, *47*, 10990−10992.

(26) Zhou, J.; Amrane, S.; Korkut, D. N.; Bourdoncle, A.; He, H. Z.; Ma, D. L.; Mergny, J. L. Combination of i-Motif and G-Quadruplex Structures within the Same Strand: Formation and Application. *Angew. Chem., Int. Ed.* **2013**, *52*, 7742−7746.

(27) Engelhard, D. M.; Pievo, R.; Clever, G. H. Reversible Stabilization of Transition-Metal-Binding DNA G-Quadruplexes. *Angew. Chem., Int. Ed.* **2013**, *52*, 12843−12847.

(28) Jin, B.; Zhang, X.; Zheng, W.; Liu, X. J.; Qi, C.; Wang, F. Y.; Shangguan, D. H. Fluorescence Light-Up Probe for Parallel G-Quadruplexes. *Anal. Chem.* **2014**, *86*, 943−952.

(29) Li, T.; Dong, S. J.; Wang, E. K. A Lead(II)-Driven DNA Molecular Device for Turn-On Fluorescence Detection of Lead(II) Ion with High Selectivity and Sensitivity. *J. Am. Chem. Soc.* **2010**, *132*, 13156−13157.

(30) Kotch, F. W.; Fettinger, J. C.; Davis, J. T. A Lead-Filled G-Quadruplex: Insight into the G-Quartet's Selectivity for Pb^{2+} over K^{+}. *Org. Lett.* **2000**, *2*, 3277−3280.

(31) Han, D. M.; Ma, Z. Y.; Zhao, W. W.; Xu, J. J.; Chen, H. Y. Ultrasensitive Photoelectrochemical Sensing of Pb^{2+} Based on Allosteric Transition of G-Quadruplex DNAzyme. *Electrochem. Commun.* **2013**, *35*, 38−41.

(32) Markad, G. B.; Battu, S.; Kapoor, S.; Haram, S. K. Interaction between Quantum Dots of CdTe and Reduced Graphene Oxide: Investigation Through Cyclic Voltammetry and Spectroscopy. *J. Phys. Chem. C* **2013**, *117*, 20944−20950.
(33) Lightcap, I. V.; Kamat, P. V. Fortification of CdSe Quantum Dots with Graphene Oxide. Excited State Interactions and Light Energy Conversion. *J. Am. Chem. Soc.* **2012**, *134*, 7109−7116.
(34) Sun, S. M.; Wang, W. Z.; Zhang, L. Bi_2WO_6 Quantum Dots Decorated Reduced Graphene Oxide: Improved Charge Separation and Enhanced Photoconversion Efficiency. *J. Phys. Chem. C* **2013**, *117*, 9113−9120.
(35) Wang, Y.; Lu, J.; Tang, L. H.; Chang, H. X.; Li, J. H. Graphene Oxide Amplified Electrogenerated Chemiluminescence of Quantum Dots and Its Selective Sensing for Glutathione from Thiol-Containing Compounds. *Anal. Chem.* **2009**, *81*, 9710−9715.
(36) Chen, D.; Feng, H. B.; Li, J. H. Graphene Oxide: Preparation, Functionalization, and Electrochemical Applications. *Chem. Rev.* **2012**, *112*, 6027−6053.
(37) Zhao, W. W.; Ma, Z. Y.; Yan, D. Y.; Xu, J. J.; Chen, H. Y. In Situ Enzymatic Ascorbic Acid Production as Electron Donor for CdS Quantum Dots Equipped TiO_2 Nanotubes: A General and Efficient Approach for New Photoelectrochemical Immunoassay. *Anal. Chem.* **2012**, *84*, 10518−10521.
(38) Zeng, X. X.; Ma, S. S.; Bao, J. C.; Tu, W. W.; Dai, Z. H. Using Graphene-based Plasmonic Nanocomposites to Quench Energy from Quantum Dots for Signal-On Photoelectrochemical Aptasensing. *Anal. Chem.* **2013**, *85*, 11720−11724.
(39) Xie, G. C.; Zhang, K.; Fang, H.; Guo, B. D.; Wang, R. Z.; Yan, H.; Fang, L.; Gong, J. R. A Photoelectrochemical Investigation on the Synergetic Effect between CdS and Reduced Graphene Oxide for Solar-Energy Conversion. *Chem.—Asian J.* **2013**, *8*, 2395−2400.
(40) Bell, N. J.; Yun, H. N.; Du, A. J.; Coster, H.; Smith, S. C.; Amal, R. Understanding the Enhancement in Photoelectrochemical Properties of Photocatalytically Prepared TiO_2-Reduced Graphene Oxide Composite. *J. Phys. Chem. C* **2011**, *115*, 6004−6009.
(41) Zhang, B. T.; Lu, L. L.; Hu, Q. C.; Huang, F.; Lin, Z. ZnO Nanoflower-based Photoelectrochemical DNAzyme Sensor for the Detection of Pb^{2+}. *Biosens. Bioelectron.* **2014**, *56*, 243−249.
(42) Li, M.; Zhou, X. J.; Guo, S. W.; Wu, N. Q. Detection of Lead(II) with a "Turn-On" Fluorescent Biosensor Based on Energy Transfer from CdSe/ZnS Quantum Dots to Graphene Oxide. *Biosens. Bioelectron.* **2013**, *43*, 69−74.
(43) Zhao, X. H.; Kong, R. M.; Zhang, X. B.; Meng, H. M.; Liu, W. N.; Tan, W. H.; Shen, G. L.; Yu, R. Q. Graphene-DNAzyme Based Biosensor for Amplified Fluorescence "Turn-On" Detection of Pb^{2+} with a High Selectivity. *Anal. Chem.* **2011**, *83*, 5062−5066.
(44) Xiao, Y.; Rowe, A. A.; Plaxco, K. W. Electrochemical Detection of Parts-per-Billion Lead via an Electrode-Bound DNAzyme Assembly. *J. Am. Chem. Soc.* **2007**, *129*, 262−263.
(45) Shen, L.; Chen, Z.; Li, Y. H.; He, S. L.; Xie, S. B.; Xu, X. D.; Liang, Z. W.; Meng, X.; Li, Q.; Zhu, Z. W.; Li, M. X.; Le, X. C.; Shao, Y. H. Electrochemical DNAzyme Sensor for Lead Based on Amplification of DNA-Au Bio-Bar Codes. *Anal. Chem.* **2008**, *80*, 6323−6328.
(46) Zhu, X.; Lin, Z. Y.; Chen, L. F.; Qiu, B.; Chen, G. N. A Sensitive and Specific Electrochemiluminescent Sensor for Lead Based on DNAzyme. *Chem. Commun.* **2009**, *40*, 6050−6052.
(47) Miao, X. M.; Ling, L. S.; Shuai, X. T. Ultrasensitive Detection of Lead(II) with DNAzyme and Gold Nanoparticles Probes by Using a Dynamic Light Scattering Technique. *Chem. Commun.* **2011**, *47*, 4192−4194.
(48) Liu, W.; Zhu, H.; Zheng, B.; Cheng, S.; Fu, Y.; Li, W.; Lau, T. C.; Liang, H. J. Kinetics and Mechanism of G-Quadruplex Formation and Conformational Switch in a G-Quadruplex of PS2.M Induced by Pb^{2+}. *Nucleic Acids Res.* **2012**, *40*, 4229−4236.